Original Research Article

On the Modeling of causative and dependence relationship of Cancers based on Gender and Cumulative Incidence.

Abstract

Objectives
The goal of our study was to model the causative relationship and dependence of morbidity, mortality, and cumulative incidence with respect to GLOBOCAN 2020 Age Standardized World Estimates for female and male malignancies using two adjustable parameters having physical significance.

Method
The GLOBOCAN Age Standardized World Estimates for patients for the year 2020 were used in this investigation. All men and women who have received a cancer diagnosis anywhere in the world were included in the study. For the purposes of analyzing descriptive and analytical data, Kaleidagraph and Origin Softwares were employed. Bivariate empirical cross correlation and dependency analyses was used to model how the variables were related to one another.Cancer rank was investigated and utilized to shed light on probable cancer-related traits in order to assess the severity of the disease. The ratio of new cases to fatalities was calculated using equations comparing the stages of various malignancies.

Results:
In this work, the usage of a two-state parameter resulted in the estimation of the optimal solution. The rate at which female cancer cases rise relative to male cancer cases was taken into consideration by the model. When the number of male cancer cases reaches exceptionally high levels, it has been noticed that the number of female cancer cases virtually hits a limiting value. A change in curvature, pointing to an existent inflection point, was determined in the estimates for the cumulative risk of cancer incidences in both sexes. The results demonstrated a non-linear correlation with a progressive increase when the cumulative risk of cancer death for each sex was examined separately versus the global cumulative risk of cancer mortality for both sexes. Males experienced the increase more dramatically than females. This finding suggests that the global male-to-female population ratio is not the only factor contributing to cumulative risk.

Conclusion: South-Eastern Asia, out of all the regions of the world examined in this study, reached its inflection point at (16.23, 14.87), according to our built-in empirical models. This generates the baseline and standard against which the overall risk of other countries can be measured. The global cumulative risk, which was estimated as 21.50 for females and 17.94 for males, respectively, dropped at this inflection point.

Keywords: Cancer, GLOBOCAN, Cumulative Incidence, Mortality, Age Standardised

Introduction

Until recently, there was a scarcity of data on the global distribution of cancer in specific communities and countries. We now have a solid foundation to estimate the worldwide cancer burden. High incidence rates for some tumor types – colorectal, prostate, and breast cancer

were originally exclusive to North America, Western Europe, and Australia, but now they are increasing in many other nations. Lung cancer has long been recognized as a global scourge, even though its high frequency was once considered limited to high-income countries. Low-income countries used to have a higher incidence of stomach, liver, and cervical cancers, but variations in incidence over time for these and other cancer types show heterogeneity between countries. Finally, there are significant differences in cancer mortality between countries or regions, with an increasing burden in low and middle-income countries due to low optimal implementation of preventive measures and a diagnosis at a later stage of cancer development rather than an early stage. The cumulative mortality risk from cancer among African women in 2020 is roughly comparable to the rates observed among women in Northern America and Europe's highest-income countries (Stewart et al., 2003; Wild et al., 2021).

Cancerof the breast is preceded by that of the lung in Australia/New Zealand, Northern Europe, Northern America, and China (part of Eastern Asia), whereas cervical cancer is preceded by breast cancer in numerous Sub-Saharan African countries regarding disease fatality. Mortality rates in Sub-Saharan African countries has risen spontaneously and currently rank among the highest in the World. This is as a result of lack of health infrastructure and poor survival outcomes.
In 12 Sub-Saharan African countries , 5-year age-standardized relative survival assessment shows a mortality rate of 66% for cases detected between 2008 and 2015, compared to 85 to 90% for patients diagnosed in high-income countries (Joko-Fru et al., 2020; Allemani et al., 2018).

Overall, the global burden of cancer incidence and death is quickly increasing, resulting in population aging and growth, and changes in the prevalence and distribution of the cancer risk factors. Cancerous disease, a cause of premature death, has been weighed in terms of how itsaffects social and economic development levels of a nation.
In 2020, Asia accounted for half of all cancer diagnoses and 58.3 % of deaths for both sexes, with Asia accounting for 59.5 % of the global population. Despite accounting for 9.7% of the worldwide population, Europe contributes 22.8 % of all cancer cases and 19.6 % of cancer deaths, followed by the Americas with 20.9 % of incidence and 14.2 % of mortality. Because of the distinct distribution of cancer types and more excellent case fatality rates in these regions, the share of cancer fatalities in Asia (58.3%) and Africa (7.2%) is larger than the share of incidence (49.3 % and 5.7 % respectively). Breast cancer is the most frequently diagnosed cancer in women and the leading cause of death, followed by colorectal and lung in incidence and mortality respectively. Lung (11.4 %), colorectal (10.0 %), prostate (7.3 %), and stomach (5.6 %) cancers are the most often diagnosed cancers in women (11.7 % of total cases). Lung cancer is the most common type, accounting for 18.0% of all cancer fatalities, followed by colorectal (9.4%), liver (8.3%), stomach (7.7%), and female breast (6.9%). Lung cancer is the most common cause of death in men, followed by prostate and colorectal in terms of incidence and liver and colorectal in terms of mortality (Sung et al., 2021, Wild et al., 2021).

There is significant global variability in main cancer types, particularly in terms of incidence in males (8 types), and death in both men (8 types) and women (7 types). Prostate cancer is the most common in men in 112 nations, followed by lung in 36 countries, colorectal in 36 countries, and liver in 11 countries. In terms of mortality, lung cancer is the top cause of death in men in 93 countries, owing to its high fatality rate. Prostate (48 countries) and liver cancers (48 countries) are the following leading causes of death in males (23 countries). In contrast to men, breast (159 nations) and cervical cancers (23 of 26 countries) are women's most

commonly diagnosed cancers. In comparison to men, breast (159 nations) and cervical (23 of the remaining 26 countries) are women's most commonly diagnosed cancers. Breast and cervical cancers are the top causes of death in 110 and 36 nations respectively, and lung is the leading cause of death in 25 countries. For men and women, incidence rates tend to increase with increasing HDI levels, ranging from 104.3 and 128.0 per 100,000 in low HDI countries, and from 335.3 and 267.6 per 100,000 in soaring HDI countries. In men, higher HDI countries (122.9-141.1 per 100,000) had roughly 2-fold higher mortality rates than lower HDI countries (76.7-78.0 per 100,000), whereas women have minimal difference across HDI levels (67.0-88.4 per 100,000), (Sung et al., 2021; Wild et al., 2021).

In 2020, men had a 19 % higher overall cancer incidence rate (222.0 per 100,000) than women (186 per 100,000); however, rates varied significantly across areas. Incidence rates for men varied almost 5-fold, from 494.2 per 100,000 in Australia/New Zealand to 100.6 per 100,000 in Western Africa, while rates for women varied nearly 4-fold, from 405.2 per 100,000 in Australia/New Zealand to 102.5 per 100,000 in South Central Asia. These variances are primarily due to differences in risk factors and malignancies associated with them (the cancer mix) and impediments to high-quality cancer prevention and early detection.

Cancer mortality is twice as high in males as in women, with death rates 43 % higher in men than in women (120.8 and 84.2 per 100,000 respectively), owing to disparities in cancer type distribution. Men's death rates ranged from 165.6 per 100,000 in Eastern Europe to 70.2 per 100,000 in Central America, while women's death rates ranged from 118.3 per 100,000 in Melanesia to 63.1 per 100,000 in Central America and South Central Asia. Eastern Africa (11.0 %) had a greater cumulative risk of dying from cancer among women in 2020 than Northern America (8.2%), Western Europe (8.8%), and Australia/New Zealand (7.4%) (Sung et al., 2021, Wild et al., 2021).

Descriptive Analysis of World Cancers by Regions

It is crucial to consider what constitutes human development and how it might be assessed while examining cancer patterns and trends. The Human Development Index (HDI) is a composite index that measures three essential aspects of human development; life expectancy at birth, education (based on average and predicted years of schooling), and an acceptable standard of living (based on gross national income per capita). The four (or three) tiers of HDI can be used to categorize countries' development levels: low, medium, high, and extremely or increasing HDI. Cancer is the first or second major cause of premature mortality (i.e., between the ages of 30 and 69 years) in 134 of the 183 nations studied, it ranks third or fourth in more than 45 countries. Cancer is the leading cause of premature death in countries with high or very high HDI rating. Most of these countries include Canada and the United States in North America, Argentina and Chile in South America, France, Germany, and the United Kingdom in Europe, Australia and New Zealand in Oceania, and Japan, the Republic of Korea, and Singapore in Asia. It is also the leading cause of death in Thailand and Vietnam, and the second biggest cause of death in Brazil, China, and many nations in Eastern Europe (including the Russian Federation and Ukraine), as well as Algeria and Egypt, after cardiovascular disorders (Wild et al., 2020).

Cancer is ranked third or fourth in most countries in Sub-Saharan Africa, with only a few countries in the region ranking fifth or sixth. Poverty-related Non-Communicable Diseases (NCDs) such as infection-related cancers (including stomach cancer, liver cancer, and cervical cancer), cardiovascular diseases due to fetal and childhood malnutrition, and respiratory

diseases linked to a poor living environment are all more common in low-income countries (Wild et al., 2020).

Overview of Global Incidence and Mortality Trends of Major Cancer Types

Lung cancer rates have been rising in Australia, Japan, the United Kingdom, and the United States, with a peak and a subsequent fall most noticeable in the United Kingdom and the United States. Lung cancer incidence and mortality rates in males vary by country, but they are almost always linked to the prevalence of tobacco smoking 20– 30 years prior. Women's smoking epidemics often started later or not in some nations, as evidenced by the matching rates. In terms of incidence (2.1 million new cases in 2018) and mortality (1.8 million deaths in 2018), lung cancer is the most frequent cancer type worldwide. Tobacco smoking is the leading cause of lung cancer, accounting for 63 % of all lung cancer deaths globally and more than 90 % of lung cancer fatalities in countries where both men and women smoke (GBD, 2015, Lortet-Tieulent, 2014).

Breast cancer is the most frequent disease in women (2.1 million new cases in 2018) and the leading cause of cancer death in women (627 000 deaths in 2018). Breast cancer incidence rates are rapidly increasing in Asian countries (e.g., India, Japan, Thailand, and Turkey) and Latin American countries (e.g., Costa Rica and Ecuador). The shifting prevalence and distribution of various reproductive and hormonal parameters can be attributed partly to the increased incidence rates observed in many higher-income nations over the last five decades – and more recently in lower-income countries. Incidence rates have stabilized in countries with high HDI (e.g., Australia, Canada, the United Kingdom, and the United States), following a sharp drop in incidence beginning around 2000, which is thought to be the result of the publication of two landmark studies on the harmful effects of menopausal hormone replacement therapy on breast cancer risk. Many nations with high HDI have seen a consistent drop in breast cancer mortality. Notably, are Australia, Canada, and the United States, where breast cancer mortality rates dropped from 22% to 18% from 2002 to 2012 (Bray et al., 2018; Torre et al., 2017; Arnold et al., 2015).

With an expected 1.3 million new cases in 2018, prostate cancer is currently the second most frequent in men worldwide, accounting for 13.5 % of all new cases in males. It is a less common cause of cancer death, accounting for 360 000 fatalities in 2018 (6.7 % of all deaths in men). Prostate cancer incidence rates in the United States steadily rose until the mid-1990s, partly due to the development of prostate-specific antigen (PSA) testing as a diagnostic test for asymptomatic prostate cancer. By 2000, there had been a peak and the subsequent decrease. In Australia and Canada, similar time trends were seen, with incidence rates declining later. In several Asian (e.g., Turkey) and Latin American (e.g., Costa Rica and Ecuador) countries, rising incidence rates and stabilizing trends were seen. Although it is doubtful that genetic variables explain much of the trends observed in different populations, prostate cancer incidence rates are substantially higher in Black communities, implying a role for genetic factors (Zhou et al., 2016; Sierra et al., 2016).

Cervical cancer is the fourth most frequent malignancy in women worldwide, with an estimated 570 000 new cases and 311 000 deaths in 2018. Cervical cancer incidence and mortality rates have decreased in most countries over the last few decades, and the rates appear to have stabilized in many countries with high HDI (e.g., Australia, Canada, the United Kingdom, and the United States), where declines have been attributed to the success of cytology-based screening programs. However, multiple studies have found that, despite general declines in incidence and mortality rates, younger generations of women in several

countries, such as Finland and the Netherlands, have seen rises (Plummer et al., 2016; Vaccarella et al., 2013; Vaccarella et al., 2017).

Method

The goal of this work was to simulate global and regional cancer incidence and death data using GLOBOCAN 2020 estimations (https://gco.iarc.fr/today/home). This study made use of the GLOBOCAN Age Standardized World Estimates for patients for the year 2020. The study covered all men and women who had been given a cancer diagnosis anywhere in the world. Utilizing Kaleidagraph and Origin Softwares, descriptive and analytical data were analyzed. Modeling the interrelationships between the variables was done using bivariate empirical cross correlation and dependency analysis.

Results

2.2. Causal Correlation between the Number of Incidences and the Number of Deaths

The graphical representation in Figure 1 shows the logarithm of the number of incidences ($\ln N_c$) with respect to the logarithm of the number of deaths ($\ln N_d$). The graph gives a linear dependence curve which can be expressed approximately as shown in Equation (1).

$$lnN_d = \alpha \cdot lnN_c - \beta, \quad (1)$$

Where α and β, the two adjustable parameters with an estimated optimal parameters is given by α=0.976986 and β=0.321396.

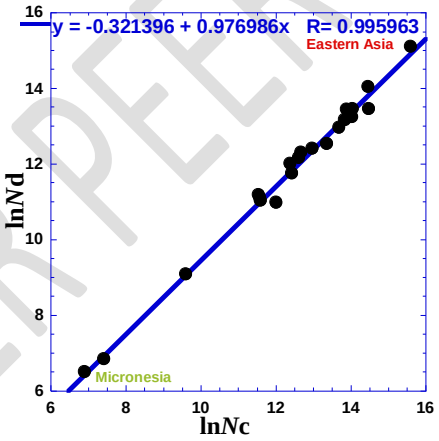

Figure 1. Correlation between Number of New Cases ($\ln N_c$) and Number of Deaths ($\ln N_d$)

To give more physical meaning to theoptimal parameters α andβinEquation 1, the Equation 1 is modified into Equation 2 by expressing the parameter β as a function of a natural log.

$$lnN_d = \alpha \cdot ln\frac{N_c}{N_{c0}} \quad (2)$$

Where α = 0.976986, From Eqs. 2, the parameter N_{c0} is taken to be the virtual limiting minimum value for the number of incidences (N_c) for which only one case of death (N_d=1) exist. Comparing Eq. 1 with Eq. 2, we can estimate the value of (N_{c0}) as follows:

$$N_{c0} = e^{\frac{\beta}{\alpha}} = 1.389532 \quad (3)$$

From Equations 2 and 3, it can be shown that the value of (N_{c0}) isgreater than unity and the value of (α) very close to unity gives an indication that the number of deaths is always less than the number of incidences (Fig. 1 and Eq. 1). Expressing Equation (3) as a power function that depends on number of incidences (N_c) and number of death (N_d), we obtain Equation (4)

$$N_d = \left(\frac{N_c}{N_{c0}}\right)^{\alpha} \qquad (4)$$

The Equation (4) can further be expressed as follows:

$$N_d = k \cdot {N_c}^{\alpha} \qquad (5)$$

The estimated parameter value of α =0.976986 is equivalent to a behavioral index of the incidences rate of cancer, and the tendency at which cancer may generate to death. The parameters α and β are dimensionless. The estimated parameter value of k =0.72514 using Equation (3) also give a fair indication that the estimated coefficients are consistent (Table 1). Thus, the estimated value of (k) being less than unity signifies that the number of deaths (N_d) is less than the number of incidences (N_c).

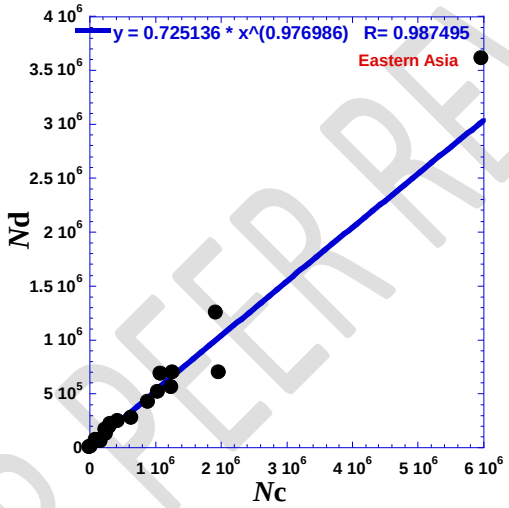

Figure 2. Power Dependence Plot of Cancer Incidences Cases

Figure 2 shows the power dependence plot of cancer incidences Cases of number of incidences against number of deaths. The dependence on power was observed to be low between the number of cancer incidences (N_c) and the number of cancer deaths (N_d). The solid line shows the dependence fit line between cancer incidences (N_c) and cancer deaths (N_d). Examining each sex separately, a correlation plot of cancer incidences (N_c) and cancer deaths (N_d) for each sex were determined. Fig. 3, shows approximately the power law dependence between the number of cancer incidences (N_{ci}) and the number of cancer deaths (N_{di}) of each sex separately. Figure (3a) represent male whilst Figure (3b) represent female. Table 1 gives values of the corresponding optimal adjustable parameters using Eq. (1), Eq. (4), and Eq. (5).

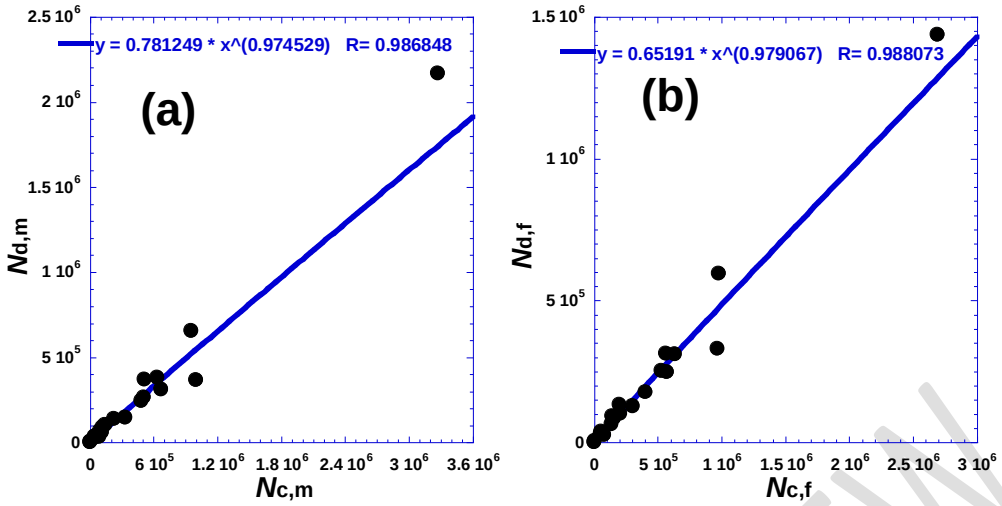

Figure 3. Correlation Plot for the Number of Cancer Incidences (N_c) and Deaths (N_d).

From the correlation plot, Fig. 3(a) represent the number of Cancer Incidences (N_c) and Cancer Deaths (N_d) for male cases whilst Fig. 3(b) also represent the represent number of Cancer Incidences (N_c) and Cancer Deaths (N_d) for female cases. The power dependence plot is represented by a solid line, and was derived from the power law equation (Eq. 5).

Table 1. Optimal Adjustable Parameters Values

Correlation	α	β	N_{c0}	k
Both sexes	0.976986	0.321396	1.389532	0.72514
Males	0.974529	0.246861	1.288287	0.78125
Females	0.979067	0.427849	1.548051	0.65191

It can be inferred from Table 1 that the low value of (k) in the female case is as a result of the increase in the number of deaths and its corresponding increase in the incidences of female cases. This in turn makes it much slower or less reactive than that of the males' situation for predicting cancer incidence. Due to the causal correlations mentioned in Fig.2, Fig.3, and Table 1 above, we thought of also revealing the correlations between cross-variables. For example, if we have a certain number of male incidences, how one could determine its corresponding incidences for females, and likewise for deaths. Fig. 4 illustrates these cross dependencies.

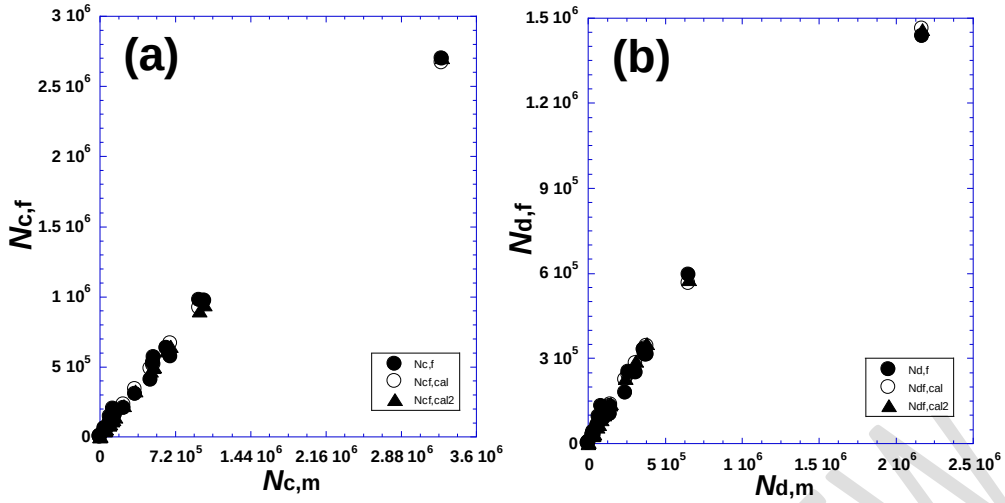

Figure 4. Mutual Correlation Plot

Figure 4 shows a mutual correlation plot between female-male cancer cases. Figure (4a) depicts the number of incidences (N_{ci}), and Figure (4b) the number of deaths (N_{di}) for the world cancer data (Globocan, 2020). The negative curvature of the observed data points trend in Fig.4 inspires us to assume the following exponential dependence.

$$N_{c,f} = N_{c,f0}(1 - e^{-\nu_c N_{c,m}}) \qquad (6)$$

$$N_{d,f} = N_{d,f0}(1 - e^{-\nu_d N_{d,m}}) \qquad (7)$$

Where ($N_{i,f0}$) and (ν_i) are two adjustable parameters. Table 2 presents the values of optimal adjustable parameters. The OAP values-1 was obtain using Equations (6) and (7), whereas the OAP values-2 was obtain using Equations (8) and (9). The Estimated Optimal Adjustable Parameters (OAP) Values and their corresponding parameters are indicated in Table 2 below.

Table 2. Estimated Optimal Adjustable Parameters (OAP) Values

Correlation	$N_{c,f0}$	ν_c	$1/\nu_c$	$N_{d,f0}$	ν_d	$1/\nu_d$
OAP Values-1	6.7×10^6	1.55×10^{-7}	6.45×10^6	2.75×10^6	3.5×10^{-7}	2.86×10^6
OAP Values-2	8.3×10^6	1.205×10^{-7}	8.3×10^6	2.55×10^6	3.92×10^{-7}	2.55×10^6

From Table 2, it can be observed that the inverse of the parameter (ν_i) is very close to the corresponding value of ($N_{i,f0}$). Re-optimising the fit to have a new model with only one adjustable parameter ($N_{i,f0}$), Equations (6) and (7) can be expressed as follows:

$$N_{c,f} = N_{c,f0}(1 - e^{-\frac{N_{c,m}}{N_{c,f0}}}) \qquad (8)$$

$$N_{d,f} = N_{d,f0}(1 - e^{-\frac{N_{d,m}}{N_{d,f0}}}) \qquad (9)$$

The optimised parameters ($N_{c,f0}$ or $N_{d,f0}$) is thus said to have a double significance value upon estimation. The Equations (8) and (9) also describe the rapidity of the increase of the number

of female cancers ($N_{i,f}$) and that of males cancers ($N_{i,m}$) for both the incidence and the death situations .

Moreover, the optimised parameters have a tendency to reach a virtual limiting value that can depict the number of cases of females ($N_{i,f}$), when the number of males ($N_{i,m}$) cases takes a very high value. It is expected that this value be approximately proportional to the global number of people of the World related to the studied year, and can increase each year according to the world population.

2.3. Cumulative Risk of the Number of New Cases and the Number of Deaths

Cumulative risk is a measure of the total risk that a certain event will happen during a given period of time. In cancer research, it is the likelihood that a person who is free of a certain type of cancer will develop that type of cancer by a specific age. In developing the cumulative risk model of cancer incidence for both sexes, a graphical representation of the cumulative risk (cum. Risk) of cancer incidences of each sex was plot separately against the global cumulative risk (Glob. cum. Risk) of cancer incidences of both sexes. Figure (5a) shows a reliable linear dependence, which can be expressed as follows:

$$Cum.\ Risk(c)_m = a_m \times Cum.\ Risk(c) \quad (10)$$

$$Cum.\ Risk(c)_f = a_f \times Cum.\ Risk(c) \quad (11)$$

It can be observed that the values of (a_m =1.08769) and (a_f =0.927023) which represent the slope of the linear regression in Fig. 5a are related to the global set of data used. The ratio (a_m/a_f), which was estimated to be greater than unity (1.1733), is mainly due to the male-female population ratio in the World.

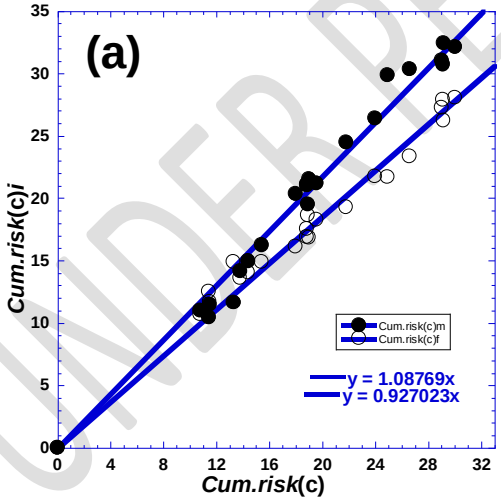

Figure 5a. Cumulative Risk of cancer Incidences of Each Sex against Both Sexes

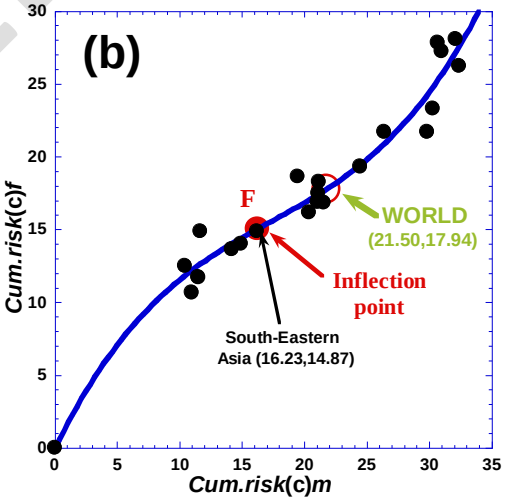

Figure 5b. Cumulative Risk (cum. Risk) of cancer Incidences of Females against Male

Fig. 5. exhibits a curvature change, which indicates an inflection point (F) coinciding with the South-Eastern Region. For the regions beyond (F), the increase of the cumulative risk (*cum.risk)* of incidences of females against the cumulative risk (*cum.risk)* of incidences of males is more accentuated comparing with the regions before (F).

However, the graphical representation of the *cum.risk* of cancer mortality of each sex separately against the global *cum.risk* of cancer mortality of both sexes (Fig. 6a) shows a non-linear dependence, and the increase is more accentuated for males than for females. This

ascertainment indicates that it is not only due to the male-female population ratio in the World.

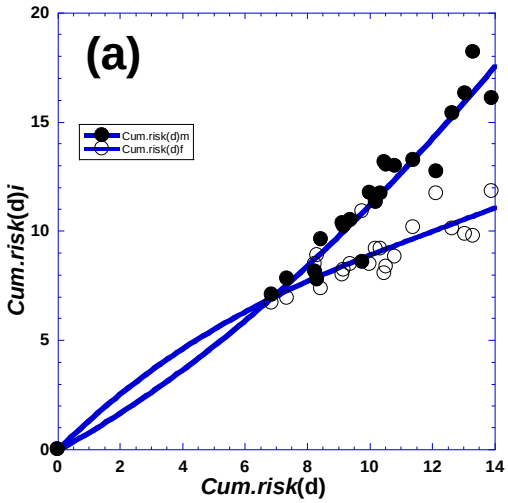

Figure 6a. Cumulative Risks of cancer Deaths of each sex against both sexes

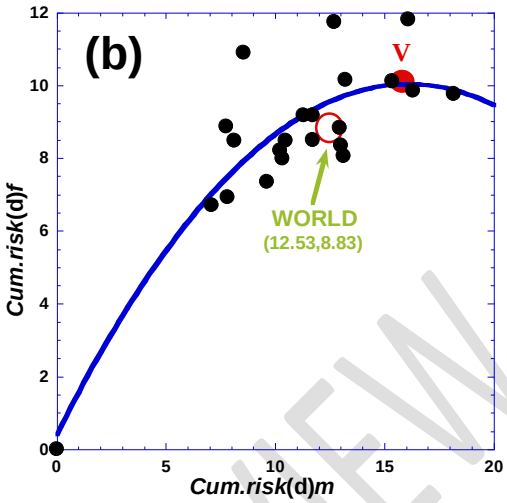

Figure 6b. Cumulative Risk of Cancer Deaths of Females against Males.

Fig. 6.b exhibits a negative curvature, which shows approximately a vertex point at point (V), indicating that for the regions beyond (V). The increase of the *cum.risk* of cancer mortality of females against the *cum.risk* of cancer mortality of males is more attenuated comparing with the regions before (F) and probably there is a pseudo-plateau.
Finally, different mortality-incidence correlations shown in Fig. 7 exhibit similar behavior characterized by a vertex point (V) showing an increase followed by a decrease

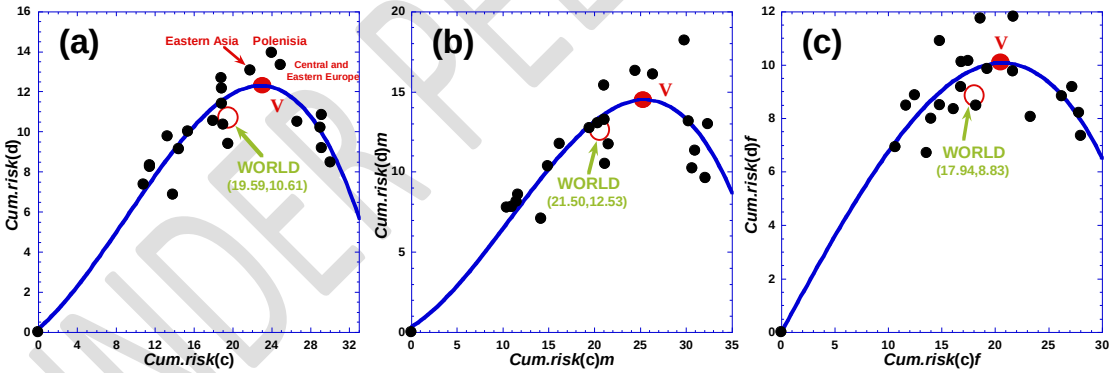

Figure 7. Mutual correlation deaths-incidences in cumulative risk; (a):the*cum.risk* of cancer deaths of both sexes against the *cum.risk* of cancer incidences of males. (b): the *cum.risk* of cancer deaths of males against the *cum.risk* of cancer incidences of males. (c): the *cum.risk* of cancer deaths of females against the *cum.risk* of cancer incidences of females.

3. Correlation male-female between the World Age-standardized rates

Firstly, the analysis of the mutual correlation (Table 1) between the World Age-Standardized Rates of females (ASR_f) and the World Age-Standardized Rates of males (ASR_m) can be fitted

into a non-linear regression for cancers for world 2020 using at least a three-degree polynomial Equation as indicated by Equation (12).

$$y = x(ax^2 + bx + c) \qquad (12)$$

Where *a*, *b*, and *c* are three adjustable parameters. We notice that we have suggested an *x*-factor as an extrapolation method to constrain the curve to pass through (0,0) to have a logical phenomenon for the two correlations. Assuming that all populations are mixed, then zero males automatically correspond to zero females. We add that the polynomial form of Eq. 12 exhibits an inflection point F(x_0,y_0) for which if we do a double shift, both in abscissa axis (x_0) and in ordinate axis (y_0), the form of Eq. 12 can be simplified in the general form expressed as follows:

$$Y = \alpha_i X(X^2 + \beta_i), \qquad (13)$$

Where the values of optimal adjustable parameters α_i, β_i, ($X = x - x_0$) and ($Y = y - y_0$), and ($x_0 = ASR_{i,0}$) and ($y_0 = ASR_{j,0}$) are presented in Tables 3 and 4. We note that the pair of data point ($ASR_{i,0}$, $ASR_{j,0}$) are the coordinates of the center of symmetry, and (Fi) is the global trend of points as shown in Fig. 8. The values ofα_i-coefficients represent the rapidity of the increase in the Age-standardized incidence rates of females with respect to the increase of the Age-standardized incidence rates of males. The factor (β_i) is a term for representing the boundary conditions.

Table 3. Age-standardized (World 2020) Incidence Rates for all Cancers.

Region	Males (*x*)	Females (*y*)
Australia and New Zealand	328.0	294.2
Western Europe	327.8	273.3
Northern Europe	313.4	282.4
Northern America	307.5	289.3
Southern Europe	301.3	241.9
Central and Eastern Europe	285.3	215.1
Polynesia	248.3	215.8
Eastern Asia	242.0	195.6
RMS	**223.10**	**197.28**
Mean	**209.59**	**188.64**
Southern Africa	208.8	178.8
World	**206.9**	**178.1**
South America	205.6	185.1
Median	**204.59**	**178.8**
Caribbean	204.5	167.6
Micronesia	202.6	165.8
Western Asia	193.2	159.5
Melanesia	180.8	193.0
Inflection point (F)	**173.06**	**159.71**
South-Eastern Asia	156.6	147.5
Northern Africa	143.3	138.4

Central America	134.6	136.3
Eastern Africa	110.2	145.0
Middle Africa	107.4	114.2
South-Central Asia	101.8	101.5
Western Africa	98.3	121.1

Cite Well: https://gco.iarc.fr/today/home.

Our empirical models can help determine the severity of cancer sickness in both men and women. Male and female incidence inflection points are 173.06 and 159.71, respectively. Male cancer rates, on average, outnumber female cancer rates. South-Eastern Asia, Northern Africa, Central America, Eastern Africa, Middle Africa, South-Central Asia, and Western Africa have not only yet to reach their inflection points in terms of cancer incidence but also have rates that are lower than the global rates of 206.9 and 178.1 for male and female cancer incidence respectively. In terms of sex, West Africa had the lowest incidence rates. The rates in Southern America, the Caribbean, Micronesia, Western Asia, and Melanesia mostly fell between the World and the estimated inflection point rates.

The plot of the World Age-Standardized Rates of females ($y = ASR_{\text{fem}}$) and the World Age-Standardized Rates of males ($x = ASR_{\text{mal}}$) is shown in Fig. 8. We note that the trend of data points permits us to formulate Eq. 14 in the form as :

$$ASR_{fem} = \alpha_1 (ASR_{mal} - ASR_{mal,0}) \left[(ASR_{mal} - ASR_{mal,0})^2 + \beta_1 \right] + ASR_{fem,0} \qquad (14)$$

Where α_1 and β_1 are two optimal parameters with positive values. The values of optimal adjustable parameters α_1, β_2, ($x_0 = ASR_{mal,0}$) and ($y_0 = ASR_{fem,0}$) are presented in Table 3. The values of α_1-coefficients represent the rapidity of the increase in the Age-standardized incidence rates of females with the increase of the Age-standardized incidence rates of males.

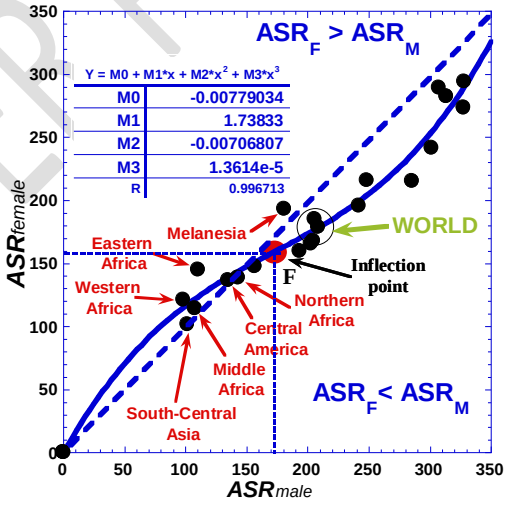

Figure 8. World Age-Standardized Rates of females (ASR_{f}) and that of males (ASR_{m})

Table 4. Optimal Adjustable Parameters Values

Correlation	α_i	β_i	x_0	y_0
Male – Female	α_1	β_1	$ASR_{\text{mal},0}$	$ASR_{\text{fem},0}$

1.3614×10^{-5}	37838.24	173.06	159.71

4. Correlation incidence-mortality between the World Age-standardized rates

Table 5. Age-standardized (World 2020) incidence and mortality rates, all cancers excl. Non-melanoma skin cancer from https://gco.iarc.fr/today/home.

Region	Incidence (x)	Mortality (y)
Australia and New Zealand	309.6	84.7
Western Europe	296.9	103.0
Northern America	296.2	86.5
Northern Europe	295.3	99.1
Southern Europe	267.6	98.4
Central and Eastern Europe	239.4	118.3
Polynesia	230.0	127.0
Vertex point (F)	**229.47**	**124.31**
Eastern Asia	215.8	122.8
RMS	**207.04**	**98.369**
Mean	**196.37**	**96.871**
South America	192.4	90.6
World	**190.0**	**100.1**
Southern Africa	187.1	107.9
Melanesia	185.3	116.9
Median	**185.30**	**-**
Caribbean	183.8	101.7
Micronesia	180.6	118.1
Western Asia	171.9	97.9
Median	**-**	**97.90**
South-Eastern Asia	150.0	94.7
Northern Africa	139.9	88.9
Central America	134.8	65.4
Eastern Africa	127.3	90.7
Western Africa	109.3	77.7
Middle Africa	109.2	77.5
South-Central Asia	101.3	66.5
Inflection point (F)	**93.82**	**57.915**

Australia and New Zealand topped the list, with incidence and mortality rates of 309.6 and 84.7, respectively, above the expected inflection point of 229.47 and 124.31 for incidence and mortality according to our empirical models' estimated parameters. Western Europe, Northern America, Southern Europe, Central and Eastern Europe, and Polynesia possess this quality after these two countries in chronological order.

All other portions of the World dropped below the Inflection point in terms of incidence and mortality, with Eastern Asia and southern America regions having rates that were halfway between the point of inflection and the global incidence and mortality rates. In addition to the seven locations mentioned, Eastern Asia and South America countries have higher incidence and mortality rates than the inflection point but are still higher than the global rates of 190 and 100.1, respectively. The closest regions below the world rates were Southern Africa and Melanesia. In other African countries, precisely the Northern, Eastern, and Central regions led the way in incidence and death rates, followed by Western Africa and Middle Africa.

However, they all fell short of the global rates. Regarding incidence and fatality rates, South-Central Asia was the least affected region.

The plot of the World Age-Standardized Rates of mortality ($y = ASR_{mor}$) and the World Age-Standardized Rates of incidence ($x = ASR_{inc}$) are shown in Fig. 9 below.
Similarly, from the previous section, using the extrapolation method, we have to constraint the curve to pass through (0,0) to have a logical phenomenon for the correlation between the World Age-Standardized Rates for mortality (ASR_{mor}) and the World Age-Standardized Rates for incidence (ASR_{inc}). Thus, it was assume that the absence of incidence automatically corresponds to zero mortality.

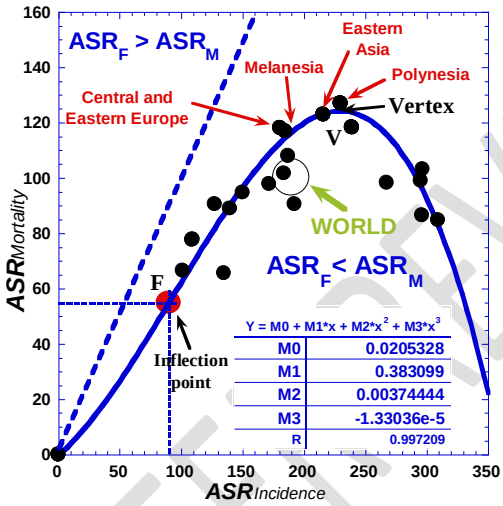

Figure 9. Correlation between the World Age-Standardized Rates for mortality (ASR_{mor}) and the World Age-Standardized Rates for incidence (ASR_{inc}). (●): Effective values for each geographical region, (○): Word average, (—): fitted values using a three-degree polynomial (Eq. 15). Dashed line represents the first bisector.

We note that the trend of data points on the graph permits us to present Eq. 15 in the form as shown by Equation (15)

$$ASR_{mor} = -\alpha_2 \left(ASR_{inc} - ASR_{inc,0}\right)\left[\left(ASR_{inc} - ASR_{inc,0}\right)^2 - \beta_2\right] + ASR_{mor,0} \qquad (15)$$

Where α_2 and β_2 are two optimal parameters with positive values. The values of optimal adjustable parameters α_1, β_2, ($x_0 = ASR_{inc,0}$) and ($y_0 = ASR_{mor,0}$) are presented in Table 4.
We note that a couple of ($ASR_{mor,0}$, $ASR_{inc,0}$) are the coordinates of the center of symmetry (F) in the global trend of data points drawn (Fig. 9). While the values of α_2-coefficient represent in a way the rapidity of the variation in the Age-standardized mortality rates with the increase of the age-standardized incidence rates. The factor (β_2) ensures the respect of the boundary conditions.
In addition, the trend of data points exhibits a vertex point V(x_2,y_2), that depicts typically a local maximum curve of curvature where the first derivative of ($y = ASR_{mor}$) with respect to ($x = ASR_{inc}$) is zero (Eq. 15). The vertex, (ASR_{mor}) increases with the increase of (ASR_{inc}), and beyond the vertex (ASR_{mor}) decreases with rise in (ASR_{inc}).

Table 6. Optimal adjustable Parameters values of (Eq. 15).

	Parameters		Inflection		Vertex	
Correlation	α_i	β_i	x_0	y_0	x_2	y_2
	α_2	β_2	$ASR_{\text{inc},0}$	$ASR_{\text{mor},0}$	$ASR_{\text{inc},0}$	$ASR_{\text{mor},0}$
Incidence – Mortality	1.33054×10^{-5}	55203.28	93.82	57.915	229.47	124.31

5. Conclusion

The cumulative incidence of male and female patients was modeled, and the dynamics of the estimates were examined, utilizing cross correlation and dependence modeling using 2020 GLOBOCAN world cancer morbidity and mortality estimates across gender.The investigation of the mutual link between cancer mortality and morbidity found a downward curve in the trend, which represents exponential dependence. To describe the rate of speed in male and female cancer incidence and mortality within the same system that accounted for correlation and dependence dynamics, two optimally adjustable parameters were introduced.The optimized parameters showed a propensity to approach a virtual limitation value that can rise annually in accordance with the worldwide population and is roughly proportional to the global incidence connected to the analyzed year. The Cumulative Risk Model of World Estimates' parameters showed non-linear dependencies.South-Eastern Asia, out of all the regions of the world examined in this study, has achieved its inflection point at (16.23, 14.87), according to our built-in empirical models. This creates the baseline and standard against which the overall danger of other countries can be measured.

References

WILDC.P, WEIDERPASS E, and STEWART B.W (2021), World Cancer Report, WHO Press, World Health Organization, 20 Avenue Appia, 1211 Geneva 27, Switzerland.

Joko-Fru WY, Jedy-Agba E, Korir A, et al. The evolving epidemic of breast cancer in sub-Saharan Africa: results from the African Cancer Registry Network. *Int J Cancer.* 2020;147:2131-2141.

Allemani C, Matsuda T, Di Carlo V, et al. Global surveillance of trends in cancer survival 2000-14 (CONCORD-3): analysis of individual records for 37513 025 patients diagnosed with one of18 cancers from 322 population-based registries in 71 countries. *Lancet.* 2018;391:1023-1075.

Stewart B.W., Kleihues P. (2003), World Cancer Report,IARCPress, International Agency for Research on Cancer, 150 cours Albert Thomas, F-69372 Lyon, France

GBD 2015 Risk Factors Collaborators (2016). Global, regional, and national comparative risk assessment of 79 behavioural, environmental and occupational, and metabolic risks or clusters of risks, 1990–2015: a systematic analysis for the Global Burden of Disease Study 2015.

Lancet. 388(10053):1659–1724. https://doi.org/10.1016/S0140-6736(16)31679-8PMID:27733284

Lortet-Tieulent J, Soerjomataram I, Ferlay J, Rutherford M, Weiderpass E, Bray F (2014). International trends in lung cancer incidence by histological subtype: adenocarcinoma stabilizing in men but still increasing in women. Lung Cancer. 84(1):13–22. https://doi.org/10.1016/j.lungcan.2014. 01.009 PMID:24524818

Bray F, Ferlay J, Soerjomataram I, Siegel RL, Torre LA, Jemal A (2018). Global cancer statistics 2018: GLOBOCAN estimates of incidence and mortality worldwide for 36 cancers in 185 countries. CA Cancer J Clin. 68(6):394–424. https://doi.org/10.3322/caac.21492PMID:30207593

Torre LA, Islami F, Siegel RL, Ward EM, Jemal A (2017). Global cancer in women: burden and trends. Cancer Epidemiol Biomarkers Prev. 26(4):444–457. https://doi.org/10.1158/1055-9965.EPI-16-0858 PMID:2822343

Arnold M, Karim-Kos HE, Coebergh JW, Byrnes G, Antilla A, Ferlay J, et al. (2015). Recent trends in incidence of five common cancers in 26 European countries since 1988: analysis of the European Cancer Observatory. Eur J Cancer. 51(9):1164–1187. https://doi.org/10.1016/j.ejca.2013.09. 002 PMID:24120180

Zhou CK, Check DP, Lortet-Tieulent J, Laversanne M, Jemal A, Ferlay J, et al. (2016). Prostate cancer incidence in 43 populations worldwide: an analysis of time trends overall and by age group. Int J Cancer. 138(6):1388–1400. https://doi.org/10.1002/ijc.29894PMID:26488767

Sierra MS, Soerjomataram I, Forman D (2016). Prostate cancer burden in Central and South America. Cancer Epidemiol. 44 (Suppl 1): S131–140. https://doi.org/10.1016/j.canep.2016.06.010 PMID:27678315

Plummer M, de Martel C, Vignat J, Ferlay J, Bray F, Franceschi S (2016). Global burden of cancers attributable to infections in 2012: a synthetic analysis. Lancet Glob Health. 4(9):e609–16. https://doi.org/10.1016/S2214-109X(16)30143-7PMID:27470177

Vaccarella S, Laversanne M, Ferlay J, Bray F (2017). Cervical cancer in Africa, Latin America and the Caribbean and Asia: regional inequalities and changing trends. Int J Cancer. 141(10):1997–2001. https://doi.org/10.1002/ijc.30901PMID:28734013

Vaccarella S, Lortet-Tieulent J, Plummer M, Franceschi S, Bray F (2013). Worldwide trends in cervical cancer incidence: impact of screening against changes in disease risk factors. Eur J Cancer. 49(15):3262–73. https://doi.org/10.1016/j. ejca.2013.04.024 PMID:23751569

Supplementary Materials

Table 1S. Cancer incidence and mortality statistics worldwide and by region (World 2020). from https://gco.iarc.fr/today/home.

Region	Incidence						Mortality					
	Bothsexes		Males		Females		Bothsexes		Males		Females	
	Newcases	Cum. risk 0-74(%)	Newcases	Cum. risk 0-74(%)	Newcases	Cum. risk 0-74(%)	Deaths	Cum. risk 0-74(%)	Deaths	Cum. risk 0-74(%)	Deaths	Cum. risk 0-74(%)
Notation	N_c	*Cum. risk*(c)	$N_{c,m}$	*Cum. risk*(c)$_m$	$N_{c,f}$	*Cum. risk*(c)$_f$	N_d	*Cum. risk*(d)	$N_{d,m}$	*Cum. risk*(d)$_m$	$N_{d,f}$	*Cum. risk*(d)$_f$
EasternAfrica	323781	13.30	123544	11.65	200237	14.87	219077	9.77	86631	8.56	132446	10.89
Middle Africa	104652	11.51	44738	11.50	59914	11.69	70877	8.26	31446	8.15	39431	8.47
Northern Africa	303199	14.44	145999	14.94	157200	14.02	189142	9.13	102783	10.34	86359	7.99
Southern Africa	108330	18.87	49541	21.11	58789	17.49	61014	11.39	29202	13.23	31812	10.15
Western Africa	242210	11.48	97742	10.45	144468	12.50	162717	8.32	69432	7.77	93285	8.87
Caribbean	108241	19.02	57009	21.54	51232	16.83	65230	10.36	35842	11.73	29388	9.18
Central America	250666	13.83	115048	14.17	135618	13.62	124644	6.87	60760	7.09	63884	6.70
South America	1040048	19.54	509712	21.20	530336	18.25	515475	9.39	263947	10.50	251528	8.47
Northern America	1970287	29.16	1000607	30.71	969680	27.85	693889	9.17	363987	10.23	329902	8.21
Eastern Asia	5968915	21.82	3274819	24.48	2694096	19.30	3605053	13.07	2168284	16.31	1436769	9.85
South-Eastern Asia	1084829	15.43	517930	16.23	566899	14.87	684018	10.01	370860	11.74	313158	8.49
South-Central Asia	1929099	10.82	953179	10.99	975920	10.68	1249821	7.36	654405	7.82	595416	6.92
Western Asia	433827	17.99	226820	20.36	207007	16.15	242774	10.55	139925	13.03	102849	8.35
Central and Eastern Europe	1269284	24.95	636705	29.84	632579	21.69	691336	13.32	379674	18.18	311662	9.76
Western Europe	1245175	29.18	674117	32.40	571058	26.24	557015	10.83	309005	12.97	248010	8.82
Southern Europe	888610	26.63	484233	30.31	404377	23.32	420082	10.49	242221	13.14	177861	8.05
Northern Europe	639194	29.03	335128	31.02	304066	27.22	274119	10.21	145687	11.31	128432	9.18
Australia and New Zealand	166845	30.05	88134	32.11	78711	28.06	57780	8.46	32096	9.62	25684	7.34
Melanesia	14846	18.91	6556	19.47	8290	18.64	8751	12.15	4133	12.72	4618	11.73
Polynesia	1668	24.02	871	26.40	797	21.71	927	13.93	521	16.09	406	11.81
Micronesia	1010	18.85	525	21.05	485	16.89	661	12.66	373	15.37	288	10.10
Low HDI	**635874**	**11.84**	**255843**	**10.80**	**380031**	**12.88**	**433641**	**8.68**	**183153**	**8.01**	**250488**	**9.34**
Medium HDI	**2302145**	**11.41**	**1121786**	**11.62**	**1180359**	**11.25**	**1502631**	**7.82**	**781667**	**8.39**	**720964**	**7.28**
High HDI	**7249438**	**19.30**	**3770938**	**21.22**	**3478500**	**17.60**	**4496483**	**12.18**	**2611021**	**14.84**	**1885462**	**9.66**
Very high HDI	**7898448**	**26.88**	**4189763**	**29.97**	**3708685**	**24.29**	**3457211**	**10.36**	**1912921**	**12.62**	**1544290**	**8.35**
World	**18094716**	**19.59**	**9342957**	**21.50**	**8751759**	**17.94**	**9894402**	**10.61**	**5491214**	**12.53**	**4403188**	**8.83**